DOI 10.1007/s11148-020-00383-6
Refractories and Industrial Ceramics *Vol. 60, No. 5, January, 2020*

SINTERED SILICON CARBIDE BASED MATERIALS: MECHANICAL PROPERTIES VS. STRUCTURE

M. V. Tomkovich,[1,2] S. N. Perevislov,[1,3,4] I. B. Panteleev,[1] and A. P. Shevchik[1]

Translated from *Novye Ogneupory*, No. 9, September, 2019

Original article submitted July 21, 2019.

The paper offers a review of literature published over the past 15 years concerning liquid-phase sintering of silicon carbide materials with various sintering activating additives. The microstructure and specifics of its formation have been investigated. The dependences of crack resistance, strength, and hardness on the material structure were studied. The relationship between the forming microstructure of the liquid-phase sintered material and its mechanical properties has been analyzed.

Keywords: silicon carbide, liquid-phase sintering, activating additives, crack resistance.

INTRODUCTION

Due to a unique combination of physical chemical, mechanical, thermal, electro-physical, tribological, corrosion and other properties, silicon carbide-based materials have been extensively used to fabricate wear-resistant, abrasive, and high-hardness products operating under high-temperature and aggressive environment conditions. One of the promising SiC-based materials, which can be sintered to high density ($\rho_{rel} \geq 98.0\%$), is liquid-phase sintered silicon carbide (LPS SiC). The main advantages of the liquid-phase sintering compared to hot-pressing and spark-plasma sintering are the possibility of obtaining materials of complex geometric shape in a broad range of dimensions without additional machining, and higher productivity of the process. However, this technique also has disadvantages, such as: 1 — sintering to obtain high degree of densification, which is accompanied by a considerable shrinkage, is technologically challenging; 2 — SiC interactions with oxides result in carbide decomposition at high temperatures and considerable loss of mass during sintering, which negatively affects the mechanical properties of the products.

Main physical and mechanical properties of LPS SiC materials as functions of a different content of the sintering activating oxide additives (yttrium-aluminum garnet (YAG) and eutectic $MgO–Y_2O_3–Al_2O_3$ (MYA) system) are presented in Table 1. The proposed review includes the most substantial studies published over the past 15 years concerning the mechanism of liquid-phase sintering, microstructure of LPS SiC materials and its effect on mechanical properties, as well as analysis of LPS SiC properties and applications.

LIQUID-PHASE SINTERING OF SILICON CARBIDE MATERIALS

Liquid-phase sintering includes three main stages: 1 — redistribution of liquid caused by the capillary forces, and rearrangement of solid particles according to the grain boundary sliding mechanism; 2 — dissolution of silicon carbide particles along the grain boundaries resulting in considerable densification and modification of the grain shape; and 3 — final stage of sintering characterized by grain coarsening via Ostwald ripening.

Densification of a porous body during sintering occurs as a result of SiC mass transfer, the intensity of which in absence of the liquid phase depends on the diffusion parameters of the sintered material, such as a diffusion (self-diffusion) coefficient and diffusion activation energy. The diffusion ac-

[1] Federal State Budgetary Educational Institution of Higher Education "St. Petersburg State Technological Institute (Technical University)," St. Petersburg, Russia.
[2] Federal State Budgetary Institution of Science "Ioffe Physical-Technical Institute of the Russian Academy of Sciences," St. Petersburg, Russia.
[3] Federal State Budgetary Institution of Science "Grebenshchikov Institute of Silicate Chemistry of the Russian Academy of Sciences," St. Petersburg, Russia.
[4] perevislov@mail.ru

tivity of the refractory covalent compounds, such as SiC, becomes noticeable only at high temperatures (>2,100°C). However, achieving such sintering temperatures is associated with economic and technological difficulties, considerable recrystallization grain growth, and partial peritectic decomposition of silicon carbide [4] according to the reaction:

$$SiC_{sol} \rightarrow Si_{gas} + C_{sol}. \quad (1)$$

As a result, the widely practiced SiC sintering activation methods included those utilizing direct application of external pressure (hot pressing, spark plasma sintering) or creation of pressure using gas atmosphere, and minimization of SiC grain size to $d_{0.5} \ll 1$ μm (application of submicron and nanosized powders). In general, the physical essence of different sintering activation techniques consists in increasing the concentration of SiC crystal defects, accelerating the diffusion processes, and facilitating the process of plastic deformation at high temperatures [5, 6].

By utilizing liquid-phase sintering, it becomes possible to compensate for a low-rate self-diffusion of SiC and obtain a dense silicon carbide material without applying external pressure. The physical and chemical principles of this activation method are based on the fact that the liquid phase, which fills the pores, contributes to the appearance of new mechanisms of mass transfer. The processes of mutual dissolution of the components, chemical interaction and high-temperature decomposition activate the atomic diffusion not only in the liquid phase, but also along the solid-liquid, gas-liquid, and gas-solid interfaces. Due to a combination of various physical and chemical processes (SiC interaction with the liquid-phase components to form gaseous volatile compounds interacting between themselves), a specific structure of the liquid-phase sintered materials is formed represented by SiC grains and intergranular phase (oxides) crystallizing from the melt during cooling [7 – 13].

By using the summarized results of predicting the thermodynamic and chemical compatibility of the components in the process of creating composite materials, the authors of Ref. [14, 15] believe that the most attractive additives, which activate the SiC sintering process, are the following: oxygen-containing Al_2O_3, BeO, Y_2O_3, La_2O_3, CaO, MgO, ZrO_2, and oxygen-free AlN.

Component Interaction during the Liquid-Phase Sintering Process

Liquid-phase sintered silicon carbide is obtained by using various sintering additives, which may include either individual compounds, such as Al_2O_3 [8, 10, 16 – 18], or dual- and triple-component oxide-based compounds, as well as compounds containing aluminum nitride. There are reports in the scientific literature about producing SiC materials using multicomponent sintering additives with the number of components $n > 3$ [19 – 24].

The most common sintering additive is a mixture of Y_2O_3 and Al_2O_3, which form yttrium aluminum garnet during sintering. Other frequently used additives besides yttrium oxide include oxides of rare-earth metals [25], as well as La, Ce, Sc, Lu, and Nd oxides [12, 26 – 29]. Also known are the additives based on the mixtures of MgO and Al_2O_3 (spinel ratio) [1]; MgO, Al_2O_3, and Y_2O_3 [30 – 33]; Al_2O_3 and CaO [34, 35]; Y_2O_3, Al_2O_3, and CaO [36], as well as component mixtures within Al_2O_3–ZrO_2 [37] and Y_2O_3–Al_2O_3–SiO_2 [6] systems. The authors of Ref. [15] have analyzed LPS SiC materials with the sintering additives containing nitrates and MgO, Al_2O_3, and Y_2O_3. Aluminum nitride is one of the few oxygen-free compounds used as a sintering additive, often in the form of an oxide mixture (e.g., Y_2O_3–AlN and AlN–Er_2O_3 [24, 38 – 42]).

Phase equilibria in most of these systems are well studied [25, 27 – 29, 38, 39, 43, 44]. The systems are described by the eutectic-type equilibrium diagrams. This means that the relationship between the melting point and concentration has a minimum, which allows lowering the liquid-phase sintering temperature. However, many of these systems contain intermediate chemical compounds, some of which melt incongruently at a temperature below the sintering temperature. Therefore, it is necessary to consider potential chemical reactions, which may take place in the process of LPS SiC heat treatment.

Chemical reactions occurring during the liquid-phase sintering process can be conditionally divided into the following two large groups:

TABLE 1. Properties of liquid-phase sintered silicon carbide materials* [1 – 3].

Composition	ρ, g/cm^3	Π, %	E_{el}, %	σ_{bend}, MPa	K_{Ic}, MPa(m$^{1/2}$	*HV*, GPa
90 wt.% SiC + 10 wt.% YAG	3.21	3.0	320	380	3.9	20.5
85 wt.% SiC + 15 wt.% YAG	3.25	2.8	390	420	4.3	19.8
80 wt.% SiC + 20 wt.% YAG	3.28	1.5	350	460	4.5	18.5
90 wt.% SiC + 10 wt.% MYA	3.23	2.0	420	510	4.1	21.0
85 wt.% SiC + 15 wt.% MYA	3.28	1.6	390	600	5.1	20.3
80 wt.% SiC + 20 wt.% MYA	3.32	1.0	350	660	4.8	19.5

* ρ) density; Π) porosity; E_{el}) modulus of elasticity; σ_{bend}) bending strength; K_{Ic}) crack resistance; *HV*) Vickers hardness.

1 — reactions of partial or complete decomposition of the initial components (e.g., Al_2O_3 and SiO_2) accompanied by the formation of unstable compounds, such as volatile suboxides;

2 — reactions leading to the formation of new stable compounds (yttrium aluminum garnet, various types of spinel, aluminates of rare-earth metals, oxynitrides, etc.) [7 – 13].

Under the actual process conditions, reactions of both groups may occur in series or in parallel, and may serve as intermediate stages of a single new phase formation process. In general, type 2 reactions may result in a loss of mass of the sintered material, appearance of concentration fluctuations, and as a consequence, non-uniform (including porous) structure. The negative effect of the loss of mass caused by these processes can be minimized by kinetically inhibiting chemical interaction, creating conditions, which prevent enhanced evaporation of the volatile components, and rationally selecting additives, which contribute to the formation of stable compounds [7 – 13].

Let us consider the reactions of decomposition in the $SiC–Y_2O_3–Al_2O_3$ system, i.e., in the process of sintering SiC in the presence of Y_2O_3 and Al_2O_3 corresponding to the yttrium aluminum garnet ratio (3:5, respectively) [7 – 13, 44 – 47]. One important advantage of the $Y_2O_3–Al_2O_3$ system is the presence of the additional three stable compounds, such as yttrium aluminum garnet $Al_5Y_3O_{12}$ (YAG), a phase with the perovskite-like structure of $AlYO_3$ (YAP), and a monoclinic $Al_2Y_4O_9$ phase (YAM). Considering the presence of a SiO_2 layer on the surface of SiC particles, which also affects the decomposition of silicon carbide, the three most likely thermodynamic reactions can be described by the following equations [44]:

$$SiC_{sol} + 2SiO_{2sol} \rightarrow 3SiO_{gas} + CO_{gas}, \quad (2)$$

$$SiC_{sol} + Al_2O_{3sol} \rightarrow Al_2O_{gas} + SiO_{gas} + CO_{gas}, \quad (3)$$

$$SiC_{sol} + Y_2O_{3sol} \rightarrow Y_2O_{gas} + SiO_{gas} + CO_{gas}. \quad (4)$$

It should be noted that SiC reactions with oxides during free sintering without applying pressure result in substantial decomposition of the components yielding gaseous SiO, Al_2O, Y_2O and CO compounds responsible for the loss of mass, formation of the porous structure of the material and, as a result, reduction in the level of mechanical properties.

Yttrium oxide is the most thermodynamically stable. It forms a smaller concentration quantity of the volatile components with silicon carbide according to reaction (4), i.e., Al_2O_3 predominantly evaporates from the melt [44]. As a result, the liquid phase becomes enriched with yttrium oxide relative to the YAG stoichiometric ratio. This phenomenon is typical when sintering materials above 1,820°C for more than 10 minutes. By increasing the partial pressure of CO as one of the gaseous products of the decomposition reaction, it becomes possible to shift the equilibrium toward the initial substances [7 – 13]. For example, as shown in [7, 8], in the process of free sintering of β-SiC with Al_2O_3 under CO pressure equal to one atmosphere (0.105 MPa), the loss of mass can be reduced by 2 to 4 times.

In practical applications, as shown in [7 – 9], even a simple technological tweak (such as a use of a partial fill) can guarantee sufficiently high partial pressure of gaseous SiO and Si in the intergranular space of the sintered samples, causing their reaction with volatile yttrium and aluminum suboxides to occur in the liquid phase, thus, resulting in the minimized losses due to component decomposition. Keeping the concentration of Al_2O_3 higher than its YAG content by using corundum partial fills also reduces the loss of mass during sintering due to an increase in Al_2O partial pressure and compensation of evaporation thereof.

The effect of the protective gas atmosphere on the processes of oxide decomposition and evaporation of the volatile components is not limited to the formation of gaseous products under the overpressure conditions. According to data presented in [1, 30, 48, 49], sintering in Ar atmosphere reduces the loss of mass by eliminating chemical interaction of solid and liquid components with nitrogen. However, the choice of gas atmosphere in each particular case requires considering such factors as the likelihood of chemical interaction between the additive components and gas medium, granular polytypism of the utilized SiC, and amount of nitrogen dissolved in solid SiC and liquid phase [47, 50]. As noted in [16], the loss of mass and oxide decomposition during sintering of SiC with 15 wt.% of Al_2O_3 in N_2 atmosphere are much lower compared to sintering in Ar atmosphere, which is associated with partial dissolution of nitrogen in the melt causing it to become more viscous. The latter also affects the wettability of the SiC surface with the melt.

The interaction between components in the systems containing aluminum nitride ($SiC–Me_xO_y–AlN$) has its own specifics. Let us consider sintering SiC with the additives from the $Y_2O_3–AlN$ system. The phase diagram of SiC–AlN indicates the formation of a metastable β-SiC phase in the temperature range of 1600 – 1800°C, designated as β′-SiC [43]. It is characterized by a significant degree of hexagonality and, due to structural proximity, is responsible for AlN solubility in SiC. The existence of solid solutions in the SiC–AlN system has been demonstrated by sintering materials using β-SiC (*3C*-polytype) and α-SiC (*2H*-polytype) powders with AlN [14]. It was established that β-SiC dissolves 1 to 2 wt.% of AlN, while the x-ray phase analysis results showed that more than 30% of the formed solid solution is related to a hexagonal syngony (*2H*-SiC polytype).

Sintering in the $SiC–Me_xO_y–AlN$ system should preferably be conducted in the atmosphere of N_2, since the excessive nitrogen pressure effectively suppresses the reaction of aluminum nitride decomposition, which eventually reduces the loss of the material mass [38, 39, 41, 42]:

$$2AlN_{sol} \rightarrow 2Al_{liq} + N_{2gas}. \quad (5)$$

However, it is impossible to completely avoid the loss of mass when sintering materials of the $SiC–Y_2O_3–AlN$ system in the atmosphere of N_2, since under these conditions it becomes possible for type (2) reactions of decomposition and reaction [40] to occur:

$$2SiC_{sol} + SiO_{2sol} \rightarrow 3Si_{gas} + 2CO_{gas}. \quad (6)$$

Hence, it can be concluded that the information about the equilibrium diagrams of oxide systems (sintering additives) and SiC makes it possible to evaluate the likelihood of certain physical and chemical processes, and account for them when developing new materials. At a LPS SiC sintering temperature, decomposition of the initial components yielding gaseous suboxides may potentially lead to a loss of mass and formation of the porous structure. However, these processes can be suppressed by performing sintering in properly selected gas atmosphere and utilizing embedding media composed of coarse fractions of SiC–*Me*O powder increasing the partial pressure of the evaporating volatile compounds.

Contact Phenomena during Liquid-Phase Sintering

The role of sintering activating additives is determined not so much by their quantity as by their effect on densification of the material and reduction of SiC grain recrystallization. The efficiency of sintering additives is determined by the uniformity of their distribution between the grains of the main phase. To ensure uniform distribution and reduced quantity, it is feasible to introduce such additives in the form of water-soluble salts and hydrates [26, 51, 52 – 54], and do so in the process of grinding the initial SiC powder [55].

One of the principal conditions for achieving successful liquid-phase sintering is the high degree of wettability of silicon carbide particles with oxide melt. This condition is satisfied only in case of a sufficiently low surface tension of the melt, while melts with high surface tension do not wet solid SiC particles well. From the energy point of view, this condition can be quantified as follows: $W_{a.m} < W_{a.s}$, i.e., in order for the melt-wetting of the SiC grain surface to be energetically favorable, the work of adhesion of the melt ($W_{a.m}$) has to be less than the work of adhesion between liquid and solid phases ($W_{a.s}$) [27, 45].

According to [28], the value of the melt-wetting angle (θ) of the solid SiC surface of the following systems: $Al_2O_3–Y_2O_3$, $Al_2O_3–Sm_2O_3$, $AlN–Y_2O_3$, $Al_2O_3–R_2O_3$, and $AlN–R_2O_3$ (where R is a rare-earth metal) at $T > 1{,}750$°C constitutes 0 to 10 degrees, which is considerably lower than the critical value of the wetting angle (90 degrees). This indicates a complete wetting of the SiC particle surface. As noted in [28], the equilibrium value of the wetting angle is achieved over the time period from 30 to 60 min, and therefore, soaking at a constant temperature for a shorter duration cannot ensure sintering to a higher density. The gas medium used in the sintering process does not significantly affect the wetting angle: the difference between the θ-values when using Ar and N_2 did not exceed several degrees.

Under the sufficient wettability conditions, the surface tension forces help rearrange particles and densify the material. Due to the capillary forces, the liquid flows over the surface of the particles, filling the intergranular spaces and pore volume, and thus, facilitating mutual rearrangement of the particles.

LPS SiC MATERIAL MICROSTRUCTURE

Structure formation in different technological environments of the process of liquid-phase sintering of SiC materials is described in detail in [56 – 58]. The grain growth and structure formation of LPS SiC materials occur according to the dissolution-recrystallization mechanism (Ostwald ripening). Generally, such mechanism can be described by the following sequence: solid phase (SiC) is partially dissolved in liquid, Si and C atoms diffuse through the liquid, and secondary SiC precipitates on the existing (primary) SiC grains [59]. It should be noted that liquid-phase sintering, which results in high degree of densification, does not require high solubility of the solid substance in the liquid phase. On the contrary, such solubility should be avoided, since it results in material deformation [60].

Based on the theory proposed by L. S. Sigl [61], the LPS SiC material microstructure is characterized by the presence of crystalline silicon carbide grains consisting of primary (SiC-grain) and secondary (SiC-boundary layer) silicon carbide, as well as an intergranular (oxide) phase, which is partially amorphous (contains glass-phase inclusions) (Fig. 1) [48].

The dissolution-recrystallization mechanism is one of the dominating mechanisms in LPS SiC materials during SiC granular structure formation. The boundary layer of the silicon carbide grains contains such elements as Y, Al, and O. The mechanism of a core-boundary layer model formation consists in the dissolution of non-equilibrium phases in liquid followed by precipitation on the primary SiC grains (core) of silicon carbide recrystallized from the melt (boundary layer). Each SiC particle becomes surrounded by a thin amorphous layer of SiO_2 film (~1 nm) [61].

There is a significant morphological grain diversity, including equiaxed grains, elongated grains, as well as bent or straight (faceted) grains, depending on the composition of the liquid phase and the initial modification of silicon carbide (α- or β-SiC) (Fig. 2) [49]. If the amount of liquid phase is about 5 vol.%, grains generally have no pronounced faceting, while aiming for a rounded shape. If the amount of liquid phase is higher, grain spherocity becomes more noticeable. If the additive content is less than 5 vol.%, grains may nucleate within zones located in between the adjacent grains (pores). This results in the most effective packing of the material [62 – 64].

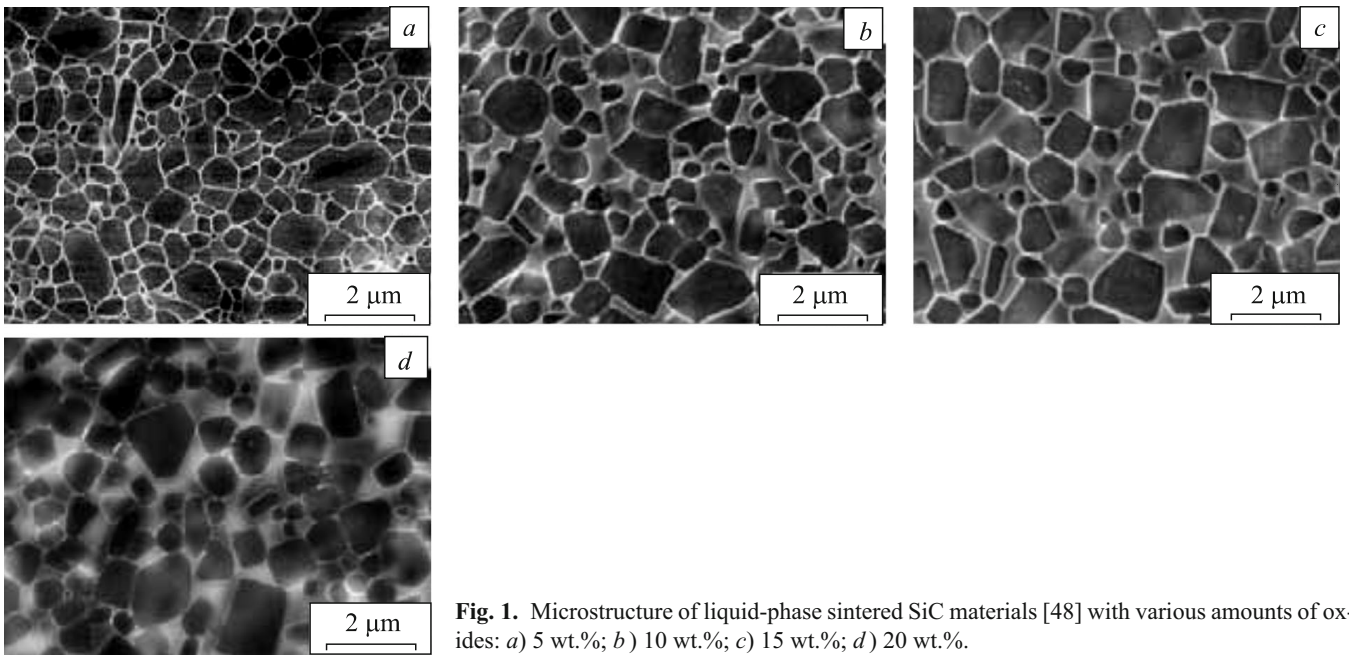

Fig. 1. Microstructure of liquid-phase sintered SiC materials [48] with various amounts of oxides: *a*) 5 wt.%; *b*) 10 wt.%; *c*) 15 wt.%; *d*) 20 wt.%.

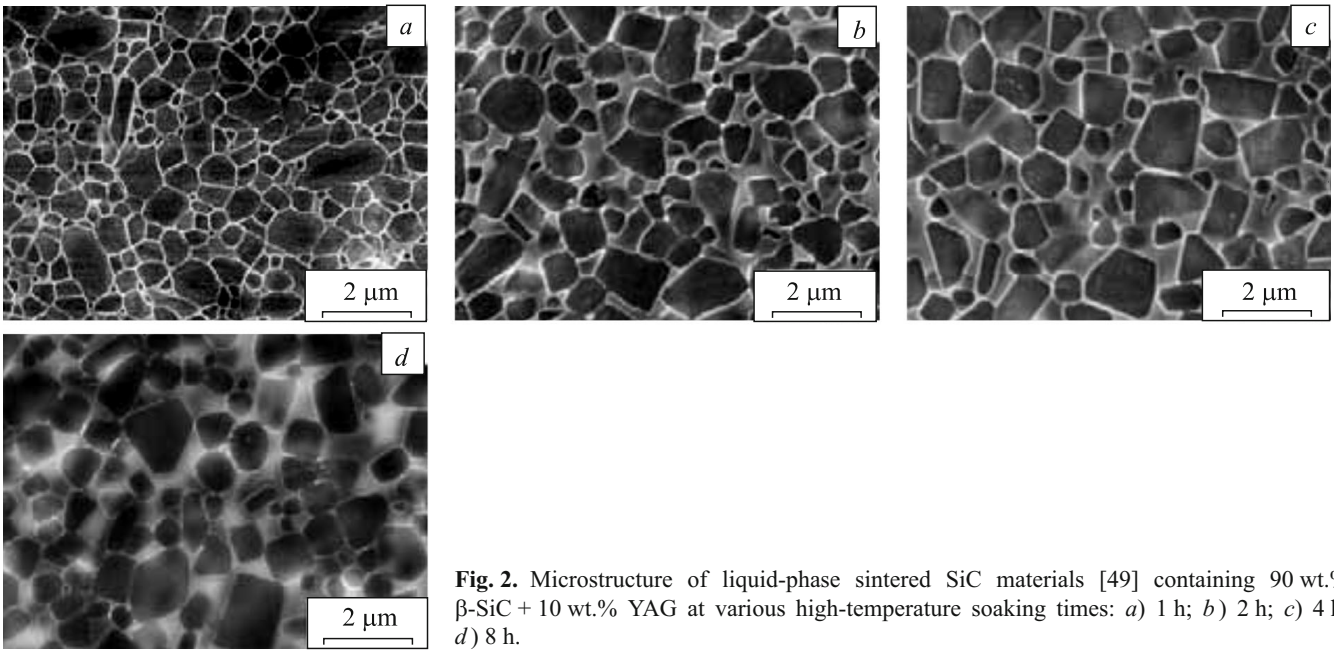

Fig. 2. Microstructure of liquid-phase sintered SiC materials [49] containing 90 wt.% β-SiC + 10 wt.% YAG at various high-temperature soaking times: *a*) 1 h; *b*) 2 h; *c*) 4 h; *d*) 8 h.

When sintering LPS SiC materials for a long time at high temperatures [49], silicon carbide grains undergo intensive growth driven by the intention to minimize the surface energy of the particles. Depending on the conditions, a normal or abnormal grain growth is observed. Normal grain growth results in narrow distribution ranges in terms of grain sizes and shapes, while abnormal growth causes a small number of large grains grow at the expense of the small grains. In this case, the grain size distribution is bimodal [65, 66].

Factors causing the abnormal grain growth include crystal anisotropy, which leads to different rates of grain growth in different directions. When the liquid phase content is high, sintered material may contain a significant amount of prismatic grains, while in case of the low oxide phase content, there is a high probability of growing elongated grains having a noticeable radius of facet curvature or plate-shaped grains having a distinct faceting [67]. Abnormal grain growth may also occur as a result of a distinct spread in the silicon carbide particle size distribution in the starting material. According to the grain growth theory [68], the growth of elongated grains is determined by the reaction along the SiC-oxides phase interface, while the growth of rounded

grains is determined by the diffusion-controlled growth of silicon carbide grains.

In the process of liquid-phase sintering of the compositions of β- and α-SiC powders, the β-SiC particles undergo a phase transition (β → α), which includes the following changes of the polymorphic modifications: $3C \rightarrow 2H$ at 1600°C, $2H \rightarrow 4H$ at 1800°C, and $4H \rightarrow 6H$ at 2000°C [43]. This means that under the standard sintering conditions of LPS SiC materials, the basic SiC phase composition includes α-polytypes 4*H*- and 6*H*-SiC, which promote more complete dissolution of SiC in the liquid phase with subsequent precipitation of the α-phase on the primary α-SiC particles. Grain growth anisotropy of the secondary α-SiC results in the formation of elongated grains demonstrating hexagonal symmetry [19, 69].

Highly interesting is the effect of nitrogen dissolution in SiC grains. Even a small amount of dissolved N_2 makes it possible to stabilize β-polytype of SiC, which helps suppressing the phase transition (β → α) [39]. In this case, a distinct decrease in the number of elongated grains is observed compared to the material structure predominantly containing α-SiC.

Correlation between Crack Resistance and LPS SiC Microstructure

Crack resistance primarily depends on the SiC grain size of the sintered material and oxide phase composition [1]. Both strength and crack resistance of the liquid-phase sintered SiC material are higher compared to the SiC materials obtained by reactive sintering. The presence of oxide phase in LPS SiC materials allows reducing the amount of defects during sintering and making such materials tougher [70]. It is believed that as a result of the difference in thermal coefficients of linear expansion (TCLE) between oxide phase and silicon carbide [37, 70, 71], crack nucleation causes weakening of the interphase bonding at the SiC grain-oxide phase interface, which affects the intensity of crack propagation along the grain boundaries. This requires higher energy compared to a trans-crystalline crack, since the path of an intergranular (inter-crystalline) crack is considerably longer. This mechanism of toughening the material is known as "crack deflection" (Fig. 3). It is mainly realized due to the presence of elongated SiC-grains in the structure [17]. The fracture toughness of such materials can be increased to 8 MPa·m$^{1/2}$ [72].

When sintering SiC materials with YAG additive, an increase in crack resistance is observed [17, 47, 71, 73, 74]. The presence of glass phases along the grain boundaries reduces the overall TCLE to approximately 3×10^{-6} K^{-1}. The liquid-phase sintering method made it possible to obtain LPS SiC materials with high fracture toughness values (K_{Ic} = 5.5 MPa·m$^{1/2}$) when using Al_2O_3–Lu_2O_3 system components as additives [29]. The aspect (length-to-diameter) ratio of the material grains was *l*:*d* = 7.

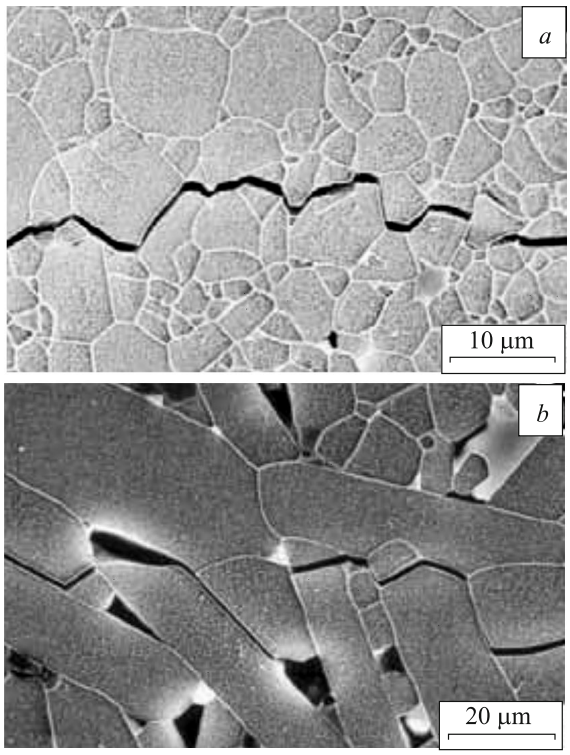

Fig. 3. Crack propagation in liquid-phase sintered SiC materials [49]: *a*) 90 wt.% α-SiC + 10 wt.% YAG, soaking time — 4 h (conventional fracture); *b*) 90 wt.% β-SiC + 10 wt.% YAG, soaking time — 8 h (fracture according to "crack deflection" mechanism).

By using a hot pressing technique, it became possible to produce β-SiC-based materials with different rare-earth oxides (Y_2O_3, Er_2O_3) along with AlN [27]. A small amount of α-SiC was introduced to the furnace charge. The materials were sintered at 1,850°C in nitrogen atmosphere. After hot pressing, subsequent heat treatment was performed at 1,850°C. It was found that the addition of AlN blocks the β → α phase transition. This, in turn, suppresses the processes of elongated hexagonal grain formation, however, the crack resistance of such materials is rather high (K_{Ic} = 6.5 MPa·m$^{1/2}$). Obviously, the high level of K_{Ic} is caused by partial dissolution of nitrogen in the melt and SiC grains, leading to the formation of a uniform dense and fine-granular structure [39].

Strength as a Function of Material Microstructure

The strength of ceramic materials is affected by the content of volumetric defects (pores, microcracks, etc.). The formation of a main crack in the material occurs when the emerging stresses exceed the force preventing the crack from growing. The Griffiths equation establishes the relationship between the strength and size of the material defects [75]:

$$\sigma = nK_{Ic}/a^{1/2}, \qquad (7)$$

where β is the strength; *n* is the geometric factor depending on the crack shape; K_{Ic} is the crack resistance; and *a* is the crack length.

To ensure high strength of LPS SiC materials, it is important to maintain a fine-granular structure throughout the sintering process. As noted above, grain growth depends on a variety of factors, but primarily on sintering temperature and isothermal time. As has been established in [47], the bending strength (σ_{bend}) of the material of the SiC–Y_2O_3–Al_2O_3 system after 4 h of sintering increases from 410 to 540 MPa, which is associated with densification of the structure in the absence of abnormal grain growth. However, after 8 h of sintering, the σ_{bend} value drops to 460 MPa due to a significant growth of the silicon carbide grains.

When sintering LPS SiC in Ar and N_2, various options of the grain growth mechanisms are realized during the dissolution-recrystallization process. When sintering is performed in Ar atmosphere, grain growth progresses with isothermal time. On the other hand, when sintering is performed in N_2 atmosphere, the grain size remains unchanged regardless of the sintering time. Such inhibition of grain growth is associated with the N_2 penetration into the oxide melt, which results in an increased surface energy at the solid-liquid interface and increased melt viscosity. These effects suppress the dissolution-recrystallization process and limit diffusion of Si and C atoms through the liquid phase, thus inhibiting grain growth [39].

One interesting technological solution consists in performing sequential sintering in the atmospheres of Ar and N_2, which yields materials with an increased σ_{bend} value as a result of higher densification during sintering in Ar and inhibited grain growth during subsequent sintering in N_2 atmosphere [16, 47, 50].

As shown in [27, 75], sintering of α-SiC with Y_2O_3 and AlN additives (as compared to YAG) results in LPS SiC material with increased high-temperature strength (at 1,200°C). The bending strength increases from 480 MPa at room temperature to 600 MPa at 1,200°C. This can be explained by softening of the intergranular viscous glass phase, which reinforces the material due to stress relaxation. However, as the temperature further increases to 1,400°C, softening of the sintering additive causes a viscous flow state of the material, which dramatically reduces its strength [27, 29, 76, 77].

As shown in [76], high-temperature heating of LPS SiC materials (to 1,200 – 1,300°C) for 0.2 h in air increases the σ_{bend} value from 440 to 1000 MPa, which can be explained by the generation of compressive stresses due to oxidation of the intergranular phase of oxynitride and YAG, and formation of γ-$Y_2Si_2O_7$ glass phase as a result of reaction between SiO_2 and YAG. These reactions reduce the strength of ceramics (at >1,400°C) due to evaporation of the formed volatile components and formation of pores in the material microstructure.

The effect of various sintering additives on the strength of hot-pressed materials after sintering and subsequent heat treatment was studied by the authors of [78]. Hot pressing was performed at 1,800°C in Ar followed by 3-hour-long heat treatment at 1,850 and 1,950°C in Ar. When using sintering additives from the Al_2O_3–La_2O_3 and Al_2O_3–Nd_2O_3 systems, the σ_{bend} values of the material increased from 500 to 650 MPa and from 550 to 610 MPa when the sintering temperature was increased from 1,800 to 1,950°C. In LPS SiC materials with oxides from the Y_2O_3–Al_2O_3 and Al_2O_3–Yb_2O_3 systems, the σ_{bend} values increased from 580 to 660 MPa and from 650 to 720 MPa when the sintering temperature was increased from 1,800 to 1,850°C. After subjecting the SiC–based materials with the Y_2O_3–Al_2O_3 and Al_2O_3–Yb_2O_3 oxide systems to heat treatment above 1,950°C, a sharp decrease in the σ_{bend} values to 440 and 370 MPa was observed. When considering the material strength in the SiC–Y_2O_3–R_2O_3 and SiC–Al_2O_3–R_2O_3 systems (where *R* is a rare-earth metal), it should be noted that the strength of LPS SiC materials drops with a decrease in ionic radius of rare-earth metals, present in the sintering additives as oxides.

Hardness as a Function of Microstructure

Hardness is the ability of the material to resist penetration of a surface force. The properties of LPS SiC materials sintered with 3 wt.% of YAG were studied and reported in [79]. In this case, three types of furnace charge with different degree of silicon carbide dispersion were used to obtain materials with different microstructure. High hardness values (27 GPa) were obtained in case of materials with the smallest grain sizes (0.5 to 1.2 μm). It has been experimentally confirmed that the hardness is inversely proportional to the square root of the mean grain size of silicon carbide [79]. Similar dependence can be seen in metals and alloys, in which the true hardness is related to the mean grain size according to the Hall-Petch equations [79]:

$$H = 3\sigma_e, \tag{8}$$

where *H* is the true hardness, and σ_e is the material plasticity;

$$\sigma_e = \sigma_0 + k/d_{0.5}^{1/2} \text{ (Hall-Petch law)}, \tag{9}$$

where σ_0 is the strength constant dependent on the grain size; *k* is the parameter dependent on the material; and $d_{0.5}$ is the mean grain size.

During hot pressing of SiC with 10 wt.% of additives, the hardness increases from 22.0 to 24.5 – 25.0 GPa after heat treatment [80], which contradicts the findings of the authors of [39]. A decrease in hardness is explained by an increased porosity resulting from the decomposition reactions, which take place during the heat treatment process [81]. The decomposition reactions lead to high losses of mass of the material, e.g., from 3.0 to 5.5 wt.%.

It was noticed that the hardness of a liquid-phase sintered SiC material decreases with an increase in YAG content from

19.3 – 20.1 GPa at 5 wt.% of YAG to 15.6 – 16.8 GPa at 25 wt.% of YAG [1, 46], which is associated with the low hardness of the intergranular phase (hardness of a hetero-phase material is subject to an additive law). A similar effect is seen when adding aluminum oxynitrides. Sintering of SiC with the additives from the Y_2O_3–AlN [40], Y_2O_3–γ-AlON [82], or AlN–γ-AlON systems results in the formation of solid solutions with SiC. The hardness of the material increases with the concentration of additives. This is explained by the fact that the hardness of the formed solid solution is higher, than that of γ-AlON [82]. When performing sintering with the additives containing γ-AlON, the hardness increases from 18.0 GPa at 10 wt.% of the additive to 28.0 GPa at 40 wt.% of the additive. After introducing 50 wt.% of γ-AlON, the hardness decreases to 24.0 – 26.0 GPa. According to [42], when performing sintering with AlN, the hardness increases from 21.2 GPa at 5 wt.% of AlN to 25.4 GPa at 25 wt.% of AlN.

APPLICATIONS OF LIQUID-PHASE SINTERED SILICON CARBIDE MATERIALS

The abrasive wear of the material decreases with hardness [83]. Therefore, a hard silicon carbide material having a fine-granular microstructure is characterized by high wear resistance. Due to these properties, silicon carbide-based materials are often used as abrasives. Silicon carbide is used to fabricate heating elements. By controlling the microstructure of LPS SiC materials, it becomes possible to adjust material resistivity, which can be useful when fabricating heating elements. LPS SiC materials can also be used as components of the diesel particulate filters for gas purification. These materials are cheaper than silicon nitride materials and have greater hardness and wear resistance compared to corundum materials. In addition, it should be noted that LPS SiC materials have special applications in thermal nuclear reactors on fast neutrons as plutonium storage containers [84]. Liquid-phase sintered silicon carbide is used to produce heat-engine components, such as valves, valve seats, piston pins, seals, etc. [84]. LPS SiC materials are used for lining grinding units (ball-mills and planetary mills), as friction units in submersible pumps for pumping abrasive liquids, as well as armor materials for protecting military personnel and equipment [86, 87].

CONCLUSIONS

By controlling a microstructure of liquid-phase sintered SiC materials using initial silicon carbide powders of different polymorphic modifications (α- and β-SiC) and different degree of dispersion, and by performing sintering under different process conditions (temperature, pressure, gas medium composition, process duration) and using sintering (multicomponent oxide and oxynitride) additives, it becomes possible to engineer various properties of the sintered materials to obtain products possessing high physical, mechanical, and operational characteristics.

REFERENCES

1. S. N. Perevislov, V. D. Chupov, and M. V. Tomkovich, “Effect of the activating additives of yttrium aluminum garnet and magnesia spinel on compactability and mechanical properties of SiC-ceramics,” *Vopr. Materialoved.*, **65**(1), 123 – 129 (2011).
2. S. N. Perevislov, I. B. Panteleev, A. P. Shevchik, and M. V. Tomkovich, “Microstructure and mechanical properties of SiC-materials sintered in the liquid phase with the addition of a finely dispersed agent,” *Refract. Ind. Ceram.*, **58**(5), 577 – 582 (2018).
3. S. N. Perevislov, A. S. Lysenkov, D. D. Titov, et al., “Production of ceramic materials based on SiC with low-melting oxide additives,” *Glass Ceram.*, **75**(9/10), 400 – 407 (2019).
4. F. Aldinger and V. A. Weberruss, Advanced Ceramics and Future Materials, Wiley (2010).
5. A. P. Garshin, V. M. Gropyanov, G. P. Zaytsev, et al., Ceramics for Machine-building [in Russian], Nauchtekhlitizdat, Moscow (2003).
6. E. Gomez, J. Echeberria, I. Iturrizab, and F. Castro, “Liquid phase sintering of SiC with additions of Y_2O_3, Al_2O_3 and SiO_2,” *J. Eur. Ceram. Soc.*, **24**(9), 2895 – 2903 (2004).
7. S. Baud, F. Thevenot, and C. Chatillon, “High temperature sintering of SiC with oxide additives. Part 2: Vaporization processes in powder beds and gas-phase analysis by mass spectrometry,” *J. Eur. Ceram. Soc.*, **23**(1), 9 – 18 (2003).
8. S. Baud, F. Thevenot, and C. Chatillon, “High temperature sintering of SiC with oxide additives. Part 3: Quantitative vaporization of SiC–Al_2O_3 powder beds as revealed by mass spectrometry,” *J. Eur. Ceram. Soc.*, **23**(1), 19 – 27 (2003).
9. S. Baud, F. Thevenot, and C. Chatillon, “High temperature sintering of SiC with oxide additives. Part 4: Powder beds and the influence of vaporization on the behaviour of SiC compacts,” *J. Eur. Ceram. Soc.*, **23**(1), 29 – 36 (2003).
10. S. Baud, F. Thevenot, A. Pisch, and C. Chatillon, “High temperature sintering of SiC with oxide additives. Part 1: Analysis in the SiC–Al_2O_3 and SiC–Al_2O_3–Y_2O_3 systems,” *J. Eur. Ceram. Soc.* **23**(1), 1 – 8 (2003).
11. J. Ihle, M. Herrmann, and J. Adler, “Phase formation in porous liquid phase sintered silicon carbide. Part 1: Interaction between Al_2O_3 and SiC,” *J. Eur. Ceram. Soc.* **25**(7), 987 – 995 (2005).
12. J. Ihle, M. Herrmann, and J. Adler, “Phase formation in porous liquid phase sintered silicon carbide. Part 2: Interaction between Y_2O_3 and SiC”, *J. Eur. Ceram. Soc.*, **25**(7), 997 – 1003 (2005).
13. J. Ihle, M. Herrmann, and J. Adler, “Phase formation in porous liquid phase sintered silicon carbide. Part 3: Interaction between Al_2O_3–Y_2O_3 and SiC,” *J. Eur. Ceram. Soc.*, **25**(7), 1005 – 1013 (2005).
14. A. Can, M. Herrmann, D. S. Mclachlan, et al., “Densification of liquid phase sintered silicon carbide,” *J. Eur. Ceram. Soc.* **26**(9), 1707 – 1713 (2006).
15. Z. H. Huang, D. C. Jia, Y. Zhou, and Y. G. Liu, “A new sintering additive for silicon carbide ceramic,” *Ceram. Int.*, **29**(1), 13 – 17 (2003).
16. K. Suzuki and M. Sasaki, “Effects of sintering atmosphere on grain morphology of liquid-phase-sintered SiC with Al_2O_3 additions,” *J. Eur. Ceram. Soc.*, **25**(9), 1611 – 1618 (2005).

17. S. K. C. Pillai, B. Baron, M. J. Pomeroy, and S. Hampshire, "Effect of oxide dopants on densification, microstructure and mechanical properties of alumina – silicon carbide nanocomposite ceramics prepared by pressureless sintering," *J. Eur. Ceram. Soc.*, **24**(12), 3317 – 3326 (2004).
18. K. Suzuki, N. Kageyama, and T. Kanno, "Improvement in the oxidation resistance of liquid-phase-sintered silicon carbide with aluminum oxide additions," *Ceram. Int.*, **31**(6), 879 – 882 (2005).
19. O. Fabrichnaya, M. Zinkevich, and F. Aldinger "Thermodynamic modelling in the ZrO_2–La_2O_3–Y_2O_3–Al_2O_3 system," *Int. J. Mater. Res.*, **98**(9), 838 – 846 (2007).
20. O. Fabrichnaya, G. Savinykh, T. Zienert, et al., "Phase relations in the ZrO_2–Sm_2O_3-Y_2O_3–Al_2O_3 system: experimental investigation and experimental modelling," *Int. J. Mater. Res.*, **103**(12), 1469 – 1487 (2012).
21. O. Fabrichnaya, G. Savinykh, G. Schreiber, et al., "Phase relations in the ZrO_2–Nd_2O_3–Y_2O_3–Al_2O_3 system: experimental study and thermodynamic modelling," *J. Eur. Ceram. Soc.*, **32**(3), 171 – 185 (2012).
22. R. Neher, M. Herrmann, K. Brandt, et al., "Liquid phase formation in the system SiC, Al_2O_3, Y_2O_3," *J. Eur. Ceram. Soc.*, **31**, 1/2, 175 – 181 (2011).
23. O. Fabrichnaya, G. Savinykh, G. Schreiber, and H. J. Seifert, "Experimental study of phase relations in the ZrO_2–La_2O_3–Y_2O_3 system," *Int. J. Mater. Res.*, **100**(11), 1521 – 1528 (2009).
24. O. Fabrichnaya, G. Savinykh, and G. Schreiber, "Phase relations in the ZrO_2–La_2O_3–Y_2O_3–Al_2O_3 system: experimental studies and phase modeling," *J. Eur. Ceram. Soc.*, **33**(1), 37 – 49 (2013).
25. K. Biswas, G. Rixecker, and F. Aldinger, "Effect of rare-earth cation additions on the high temperature oxidation behavior of LPS–SiC," *Mater. Sci. Eng. A.*, **374**(1/2), 56 – 63 (2004).
26. J. Gao, H. Xiao, and H. Du, "Effect of Y_2O_3 addition on ammono sol-gel synthesis and sintering of Si_3N_4–SiC nanocomposite powder," *Ceram. Int.* **29**(6), 655 – 661 (2003).
27. S. Guo, N. Hirosaki, H. Tanaka, et al., "Oxidation behavior of liquid-phase sintered SiC with AlN and Er_2O_3 additives between 1200°C and 1400°C," *J. Eur. Ceram. Soc.* **23**(12), 2023 – 2029 (2003).
28. S. P. Taguchi, R. M. Balestra, G. C. R. Garcia, and S. Ribeiro, "Spontaneous infiltrations of compound systems of Y_2O_3, Sm_2O_3, Re_2O_3, Al_2O_3 and AlN in SiC ceramics," *Ceram. Int.*, **36**(1), 9 – 14 (2010).
29. K. Biswas, G. Rixecker, and F. Aldinger, "Improved high temperature properties of SiC–ceramics sintered with Lu_2O_3-containing additives," *J. Eur. Ceram. Soc.*, **23**(7), 1099 – 1104 (2003).
30. S. N. Perevislov, V. D. Chupov, S. S. Ordanyan, "Properties of sintered materials based on silicon carbide micro-powders," *Vopr. Materialoved.*, **69**(1), 38 – 43 (2012).
31. S. N. Perevislov and D. D. Nesmelov, "Properties of SiC and Si_3N_4 based composite ceramic with nano-size component," *Glass Ceram.*, **73**(7/8), 249 – 252 (2016).
32. S. N. Perevislov, A. S. Lysenkov, D. D. Titov, et al., "Liquid-sintered SiC based materials with additive low oxide oxides," *IOP Conf. Series: Mater. Sci. Eng.*, IOP Publ., **525**(1), 012073 (2019).
33. S. N. Perevislov, M. V. Tomkovich, and A. S. Lysenkov, "Silicon carbide liquid-phase sintering with various activating agents," *Refract. Ind. Ceram.*, **59**(5), 522 – 527 (2019).
34. M. F. Zawrah and L. Shaw, "Liquid-phase sintering of SiC in presence of CaO," *Ceram. Int.*, **30**(5), 721 – 725 (2004).
35. A. S. Lysenkov, K. A. Kim, D. D. Titov, et al., "Composite material Si_3N_4/SiC with calcium aluminate additive," *J. Phys., Conf. Series*., IOP Publ., **1134**(1), 012036 (2018).
36. J. H. Lee, D. Y. Kim, and Y. W. Kim, "Grain boundary crystallization during furnace cooling of α-SiC sintered with Y_2O_3–Al_2O_3–CaO," *J. Eur. Ceram. Soc.*, **26**(7), 1267 – 1272 (2006).
37. U. I. Ryabkovyi and P. A. Sitnikov, "Conditions for preparation of oxide components and their effect on properties of Al_2O_3–ZrO_2–SiC composite," *Refract. Ind. Ceram.*, **44**(2), 115 – 118 (2003).
38. G. Magnani and L. Beaulardi, "Long-term oxidation behavior of liquid phase pressureless sintered SiC–AlN ceramics obtained without powder bed," *J. Eur. Ceram. Soc.*, **26**(15), 3407 – 3413 (2006).
39. K. Strecker and M. J. Hoffmann, "Effect of AlN-content on the microstructure and fracture toughness of hot-pressed and heat-treated LPS–SiC ceramics," *J. Eur. Ceram. Soc.*, **25**(6), 801 – 807 (2005).
40. M. Hotta and J. Hojo, "Inhibition of grain growth in liquid-phase sintered SiC ceramics by AlN additive and spark plasma sintering," *J. Eur. Ceram. Soc.*, **30**(10), 2117 – 2122 (2010).
41. R. M. Balestra, S. Ribeiro, S. P. Taguchi, et al., "Wetting behavior of Y_2O_3/AlN additive on SiC ceramics," *J. Eur. Ceram. Soc.*, **26**(16), 3881 – 3886 (2006).
42. K. Suzuki and M. Sasaki, "Microstructure and mechanical properties of liquid-phase-sintered SiC with AlN and Y_2O_3 additions," *Ceram. Int.*, **31**(5), 749 – 755 (2005).
43. A. Zangvil and R. Ruh, "Phase relationships in the silicon carbide — aluminum nitride system," *J. Am. Ceram. Soc.*, **71**(10), 884 – 890 (1988).
44. Z. Pan, O. Fabrichnaya, H. J. Seifert, et al., "Thermodynamic evaluation of the Si–C–Al–Y–O system for LPS–SiC application," *J. Phase Equilibr.*, **31**(3), 238 – 249 (2010).
45. N. Zhang, H. Ru, Q. Cai, et al., "Investigation of loss weight and densification of SiC–Al_2O_3–Y_2O_3 ceramic composite on sintering," *J. Rare Earths.*, **23**, 132 – 136 (2005).
46. R. Huang, H. Gu, J. Zhang, and D. Jiang, "Effect of Y_2O_3–Al_2O_3 ratio on intergranular phases and films in tape-casting α-SiC with high toughness," *Acta Mater.*, **53**(8), 2521 – 2529 (2005).
47. M. Castillo-Rodríguez, A. Muñoz, and A. Domínguez-Rodríguez, "Effect of atmosphere and sintering time on the microstructure and mechanical properties at high temperatures of α-SiC sintered with liquid phase Y_2O_3–Al_2O_3," *J. Eur. Ceram. Soc.*, **26**(12), 2397 – 2405 (2006).
48. S. N. Perevislov, V. D. Chupov, S. S. Ordanyan, and M. V. Tomkovich, "Obtaining high density silicon carbide materials by the liquid-phase sintering method in the component system SiC–Al_2O_3–Y_2O_3–MgO," *Ogneup. Tekh. Ker.*, No. 4/5, 26 – 32 (2011).
49. S. N. Perevislov, "Study of the structure and strength properties of liquid-phase sintered silicon carbide ceramics," *Deform. Razr. Mat.*, No. 5, 25 – 31 (2013).
50. A. L. Ortiz, A. Munoz-Bernabé, O. Borrero-López, et al., "Effect of sintering atmosphere on the mechanical properties of liquid-phase-sintered SiC," *J. Eur. Ceram. Soc.*, **24**(10/11), 3245 – 3249 (2004).
51. G. D. Semchenko, I. Yu. Shuteeva, A. N. Butenko, et al., Zol-gel Compositions for Multifunctional Applications [in Russian], Rainbow, Kharkov (2011).
52. S. V. Vikhman, O. A. Kozhevnikov, S. S. Ordanyan, and V. D. Chupov, "Solution-based method of producing silicon car-

bide mixture with oxide sintering activator and method of producing ceramic based thereon," Russian Federation patent 2455262, appl. No. 2010124772/03, filed June 16, 2010, publ. July 10, 2012, Bul. No. 19.
53. S. N. Perevislov, I. B. Panteleev, S. V. Vikhman, et al., "Co-precipitation of oxides from salt solution on the silicon carbide particle surface," *Ogneup. Tekh. Keram.*, No. 9, 9 – 16 (2015).
54. D. D. Nesmelov, O. A. Kozhevnikov, S. S. Ordanyan, et al., "Precipitation of the eutectic Al_2O_3–ZrO_2 (Y_2O_3) on the surface of SiC particles," *Glass Ceram.*, **74**(1/2), 43 – 47 (2017).
55. S. N. Perevislov, "Grinding silicon carbide powders in a planetary mill," *Vopr. Materialoved.*, **68**, 4, 73 – 80 (2011).
56. A. Gubernat, L. Stobierski, and P. Łabaj, "Microstructure and mechanical properties of silicon carbide pressureless sintered with oxide additives," *J. Eur. Ceram. Soc.*, **27**(2/3), 781 – 789 (2007).
57. F. Chen, Y. Yang, Q. Shen, and L. Zhang, "Macro/micro structure dependence of mechanical strength of low temperature sintered silicon carbide ceramic foams," *Ceram. Int.*, **38**(6), 5223 – 5229 (2012).
58. O. Borrero-López, A. L. Ortiz, F. Guiberteau, and N. P. Padture, "Microstructural design of sliding-wear-resistant liquid-phase-sintered SiC: an overview," *J. Eur. Ceram. Soc.*, **27**(11), 3351 – 3357 (2007).
59. S. N. Perevislov, "Mechanism of liquid-phase sintering of silicon carbide and nitride with oxide activating additives," *Glass Ceram.*, **70**(7/8), 265 – 268 (2013).
60. K. Ando, K. Furusawa, K. Takahashi, and S. Sato, "Crack-healing ability of structural ceramics and a new methodology to guarantee the structural integrity using the ability and proof-test," *J. Eur. Ceram. Soc.*, **25**(5), 549 – 558 (2005).
61. L. S. Sigl and H. J. Kleebe, "Core/rim structure of liquid-phase-sintered silicon carbide," *J. Am. Ceram. Soc.*, **76**(3), 773 – 776 (1993).
62. S. J. Dillon and M. P. Harmer, "Demystifying the role of sintering additives with "complexion"," *J. Eur. Ceram. Soc.*, **28**(7), 1485 – 1493 (2008).
63. F. Rodríguez-Rojas, A. L. Ortiz, O. Borrero-López, and F. Guiberteau, "Effect of the sintering additive content on the non-protective oxidation behavior of pressureless liquid-phase-sintered α-SiC in air," *J. Eur. Ceram. Soc.*, **30**(6), 1513 – 1518 (2010).
64. J. K. Lee, S. P. Lee, K. S. Cho, et al., "Characteristic evaluation of liquid-phase sintered SiC materials by a nondestructive technique," *J. Nucl. Mater.*, **386**, 487 – 490 (2009).
65. T. S. Suzuki, T. Uchikoshi, and Y. Sakka, "Effect of sintering conditions on microstructure orientation in α-SiC prepared by slip casting in a strong magnetic field," *J. Eur. Ceram. Soc.*, **30**(14), 2813 – 2817 (2010).
66. C. Cui, Y. T. Wang, J. G. Jiang, et al., "Microstructure of reactive sintered Al bonded Si_3N_4–SiC ceramics," *Trans. Nonfer. Metals Soc. China*, **16**, 42 – 45 (2006).
67. Y. I. Lee, Y. W. Kim, and M. Mitomo, "Microstructure stability of fine-grained silicon carbide ceramics during annealing," *J. Mater. Sci.*, **39**(11), 3613 – 3617 (2004).
68. O. H. Kwon and G. L. Messing, "Kinetic analysis of solution-precipitation during liquid-phase sintering of alumina," *J. Am. Ceram. Soc.*, **73**(2), 275 – 281 (1990).
69. K. A. Weidenmann, G. Rixecker, and F. Aldinger, "Liquid phase sintered silicon carbide (LPS–SiC) ceramics having remarkably high oxidation resistance in wet air," *J. Eur. Ceram. Soc.*, **26**(13), 2453 – 2457 (2006).
70. G. Magnani, L. Beaulardi, A. Brentari, et al., "Crack healing in liquid-phase pressureless-sintered silicon carbide – aluminum nitride composites," *J. Eur. Ceram. Soc.*, **30**(3), 769 – 773 (2010).
71. S. K. Lee, W. Ishida, V. G. Cao, and L. Lee, "Crack-healing behavior and resultant strength properties of silicon carbide ceramics," *J. Eur. Ceram. Soc.*, **25**(5), 569 – 576 (2005).
72. L. Vargas-Gonzalez, R. F. Speyer, and J. Campbell, "Flexural strength, fracture toughness, and hardness of silicon carbide and boron carbide armor ceramics," *Int. J. Appl. Ceram. Technol.*, **7**(5), 643 – 651 (2010).
73. J. M. Ma, F. Ye, C. F. Liu, et al., "Microstructure and mechanical properties of liquid phase sintered silicon carbide composites," *J. Zhej. Univ. Sci. A.*, **11**(10), 766 – 770 (2010).
74. O. Borrero-López, A. L. Ortiz, F. Guiberteau, and N. P. Padture, "Effect of liquid-phase content on the contact-mechanical properties of liquid-phase sintered α-SiC," *J. Eur. Ceram. Soc.*, **27**(6), 2521 – 2527 (2007).
75. D. Sciti and A. Bellosi, "Effects of additives on densification, microstructure and properties of liquid-phase sintered silicon carbide," *J. Mater. Sci.*, **35**, 3849 – 3855 (2000).
76. B. G. Simba, C. Santos, M. J. Bondioli, et al., "Strength improvement of LPS-SiC ceramics by oxidation treatment," *Int. J. Ref. Met. Hard Mater.*, **28**(4), 484 – 488 (2010).
77. V. D. Chupov and A. S. Kharlanov, "Strength of silicon carbide and silicon nitride based ceramic materials," *Ogneup. Tekh. Ker.*, No. 9, 16 – 18 (2006).
78. Y. Zhou, K. Hirao, Y. Yamauchi, and S. Kanzaki, "Tailoring the mechanical properties of silicon carbide ceramics by modification of the intergranular phase chemistry," *J. Eur. Ceram. Soc.*, **22**, 2689 – 2696 (2002).
79. S. Baud and F. Thevenot, "Microstructures and mechanical properties of liquid-phase sintered seeded silicon carbide," *Mater. Chem. Phys.*, **67**, 165 – 174 (2001).
80. S. Guicciardi, A. Balbo, D. Sciti, et al., Nanoindentation characterization of SiC–based ceramics," *J. Eur. Ceram. Soc.*, **27**(2/3), 1399 – 1404 (2007).
81. O. Borrero-López, A. Pajares, A. L. Ortiz, and F. Guiberteau, "Hardness degradation in liquid-phase sintered SiC with prolonged sintering," *J. Eur. Ceram. Soc.*, **27**(11), 3359 – 3364 (2007).
82. S. Mandal, A. S. Sanyal, K. K. Dhargupta, and S. Ghatak, "Gas pressure sintering of β-SiC – γ-AlON composite in nitrogen/argon environment," *Ceram. Int.*, **27**, 473 – 479 (2001).
83. I. M. Hutchings, Tribology, Friction and Wear of Engineering Materials, British Library Cataloguing in Publication Data (2017).
84. V. D. Krstic, M. D. Vlajic, and R. A. Verall, "SiC ceramics for nuclear applications," *Adv. Ceram. Mater. Eng. Mater.*, **122 – 124**, 387 – 396 (1996).
85. J. Briggs, Engineering Ceramics in Europe and the USA, Enceram. Menith Wood. UK, Worcester (2011).
86. S. N. Perevislov and I. A. Bespalov, "Shock-resistant silicon carbide based ceramic materials," *Pisma Zh. Tekh. Fiz.*, **43**(15), 73 – 78 (2017).
87. S. N. Perevislov, I. A. Bespalov, and M. V. Tomkovich, "Influence of structure modification of silicon carbide materials on their dynamic properties," *Refract. Ind. Ceram.*, **59**(4), 359 – 364 (2018).